Published in final edited form as:
Mol Cell Biochem. 2009 January ; 321(1-2): 45–52. doi:10.1007/s11010-008-9908-0.

Myocardial oxidative stress, osteogenic phenotype, and energy metabolism are differentially involved in the initiation and early progression of δ-sarcoglycan-null cardiomyopathy

Comlan Missihoun, **David Zisa**, **Arsalan Shabbir**, **Huey Lin**, and **Techung Lee**
Department of Biochemistry and Center for Research in Cardiovascular Medicine, University at Buffalo, 351 Biomedical Research Building, 3435 Main Street, Buffalo, NY 14214, USA
chunglee@buffalo.edu

Abstract

Dilated cardiomyopathy (DCM) is a common cause of heart failure, and identification of early pathogenic events occurring prior to the onset of cardiac dysfunction is of mechanistic, diagnostic, and therapeutic importance. The work characterized early biochemical pathogenesis in TO2 strain hamsters lacking δ-sarcoglycan. Although the TO2 hamster heart exhibits normal function at 1 month of age (presymptomatic stage), elevated levels of myeloperoxidase, monocyte chemotactic protein-1, malondialdehyde, osteopontin, and alkaline phosphatase were evident, indicating the presence of inflammation, oxidative stress, and osteogenic phenotype. These changes were localized primarily to the myocardium. Derangement in energy metabolism was identified at the symptomatic stage (4 month), and is marked by attenuated activity and expression of pyruvate dehydrogenase E1 subunit, which catalyzes the rate-limiting step in aerobic glucose metabolism. Thus, this study illustrates differential involvement of oxidative stress, osteogenic phenotype, and glucose metabolism in the initiation and early progression of δ-sarcoglycan-null DCM.

Keywords

Dilated cardiomyopathy; Oxidative stress; Osteogenesis; Energy metabolism

Introduction

Dilated cardiomyopathy (DCM) is a common cause of heart failure, and is the most prevalent cardiomyopathy [1]. DCM can result from myocardial infarction, myocarditis, mitochondrial dysfunction, and genetic abnormalities, representing the end result of diverse pathways [2,3]. The complex nature of DCM can be attributed in part to progressive tissue remodeling at the cellular and molecular levels of the affected heart [4,5]. While much progress has been made in the understanding of molecular genetics of DCM in the past decade, it remains incompletely elucidated how alterations occurring at the molecular level mediate the development of the disease, which often occurs in the setting of autoimmune cardio-inflammatory processes [6–8].

Identified DCM genes encode cytoskeletal, sarcomeric, mitochondrial, and membrane proteins [6]. Alterations of these proteins are thought to impact mechanical force generation/transmission, signal transduction, energy metabolism, and sarcolemmal stability [9]. For

Correspondence to: Techung Lee.

instance, mutations of the muscle-specific intermediate filament protein desmin can cause DCM exhibiting myocardial degeneration, calcium overload, and compromised respiratory chain [10,11]. Sarcomeric protein mutations can indirectly derange the energy status through inefficient myocardial energy use [12,13]. Altered energy metabolism may have a substantial role in the development of DCM since specific mutations in mitochondrial DNA have been found in DCM patients that compromise energy production [14,15]. Oxidative stress represents yet another aspect of the multi-faceted pathologic process that can be triggered by mitochondrial dysfunction and inflammatory response [7,8,16]. Although these diverse, but interrelated mechanisms are expected to act in a chronological cascade, early pathogenic events that occur prior to the manifestation of cardiac dysfunction are particularly important since these pathways can be of diagnostic and therapeutic values.

The TO2 hamster model of DCM, which is associated with δ-sarcoglycan mutation, exhibits cardiac dysfunction between 1 and 2 months of age, and later develops congestive heart failure resembling that seen in many patients [17–20]. Mouse models of δ-sarcoglycan deficiency have been created and shown to cause sarcolemmal fragility culminating in DCM [21,22]. Mutation of the human δ-sarcoglycan gene causes familial and idiopathic DCM associated with limb-girdle muscular dystrophy [23,24]. Since the hamster DCM model displays successive and uniform phases of pathophysiologic changes, it was used here to identify early biochemical and molecular alterations involved in the initiation and progression of DCM.

Materials and methods

Animals

Bio-F1B (normal control) and Bio-TO2 (DCM) male hamsters were obtained from Bio Breeders (Watertown, MA, USA). Procedures and protocols conformed to institutional guidelines for the care and use of animals in research. The number of animals used for each experiment is indicated in the figure legends.

Transthoracic echocardiography

Animals were anesthetized by intraperitoneal (ip) injection of xylazine (2 mg/kg) and ketamine (25 mg/kg), and remained semi-conscious during the measurement procedure. Multiple M-mode images were obtained from the short axis view of the left ventricle at the level of the papillary muscles with a GE Vingmed echo machine using a 10-MHz transducer. From this image, left ventricular end-systolic dimension (LVDs) and left ventricular end-diastolic dimension (LVDd) were measured. These dimensions were measured and averaged from at least two consecutive cardiac cycles.

Tissue lysate preparation

Animals received 1,000 units of heparin by i.p. injection prior to sacrifice by CO_2 narcosis. Tissues were immediately excised and rinsed in ice-cold Hank's Balanced Salt Solution several times. Blood samples (0.5 ml per animal) were immediately collected after the heart was excised. Plasma fractions were recovered after brief centrifugation. Freshly isolated tissue samples were minced and homogenized in an ice-cold lysis solution (phosphate-buffered saline supplemented with 0.1% Triton X-100). Homogenates were clarified by a 2-min spin in a refrigerated microfuge. Supernatants and pelleted membrane fractions were separated, following which the membrane fractions were resuspended in the lysis solution, and used for pyruvate dehydrogenase (PDH) and cytochrome *c* oxidase (COX) assays. Supernatants were used for lactate dehydrogenase (LDH) and alkaline phosphatase (ALP) assays. Protein concentrations were determined using the BCA protein assay method (Pierce, Rockford, IL, USA). Samples were frozen in small aliquots at −80°C.

Enzyme assays

LDH activities were determined as described in our previous study [25]. Assays were initiated by mixing 5 μl of tissue samples with 50 μl of the LDH substrate solution in a 96-well plate. The plate was incubated at 37°C for 30 min, following which LDH activities were measured by absorption at 492 nm. For ALP assay, samples (10 μl) were mixed with 0.1 ml of an ALP substrate solution (100 mM Tris pH 10.5, 2 mM $MgCl_2$, and 2.5 mM *p*-nitrophenyl phosphate) in a 96-well plate, and incubated at 37°C for 30 min. Reactions were stopped by 20 μl 1 N NaOH and measured by absorption at 412 nm. Tissue ALP activities were expressed as optical density units (412 nm) per mg proteins. The PDH and GAPDH assay kits, which is based on a coupled PDH/GAPDH and diaphorase reaction converting the chromogenic substrate *p*-iodonitrotetrazolium violet (INT) to formazan, was from Biomedical Research Service (Buffalo, NY, USA). COX activity was measured using an assay kit from Sigma (Saint Louis, MO, USA), which is based on observation of the decrease in absorbance at 550 nm of ferrocytochrome *c* caused by its oxidation to ferricytochrome *c* by cytochrome *c* oxidase.

MDA assay

The malondialdehyde (MDA) kit was purchased from Biomedical Research Service (Buffalo, NY, USA). For lipid peroxidation assays, 0.1 ml of TCA-treated plasma and tissue homogenates were incubated with freshly prepared 6.5 mg/ml thiobarbituric acid at 95°C for 30 min. Reaction products were extracted with *n*-butanol and measured at 540 nm.MDA concentrations were calculated using a molar extinction coefficient of $1.56 \times 10^5\ cm^{-1}\ M^{-1}$.

Glucose measurement

Plasma glucose was measured using the One Touch blood glucose monitoring system (Johnson&Johnson, Milpitas, CA, USA).

Multiplexed immunoassays of plasma samples

Hamster plasma samples were analyzed by Rules-Based Medicine, Inc. (Austin, TX, USA) using their rodent MAP analysis program. Plasma levels of myeloperoxidase, monocyte chemotactic protein-1, SGOT, insulin, osteopontin, and leptin were obtained using the MAP analysis.

Western blotting

Total proteins were resolved by SDS-PAGE and electro-transferred to Immobilon-P membrane as described [26]. The membrane was incubated with a 1,000-fold diluted primary antibody solution followed by washing with a saline solution supplemented with 0.025% TW-20. Secondary antibodies were conjugated with horse radish peroxidase. Protein bands were visualized using the chemiluminescent substrate system (Pierce, Rockford, IL, USA) and imaged by Fuji imager. The PDH-E1α antibody (#A-21323) and the 39-kDa subunit of Complex I antibody (#A-21344) were purchased from Molecular Probes (Eugene, OR, USA).

Statistics

Data presented were representatives of at least two separate assays, and were means ± SEM. Some error bars were too small to appear on the graph. Student's *t*-tests were used for statistical analysis.

Results

Presymptomatic and symptomatic stages of hamster DCM

Identification of early pathologic events that occur prior to the manifestation of cardiac dysfunction is of mechanistic, diagnostic, and therapeutic importance. We carried out physiological and biochemical analyses focusing on the initiation and progression of the TO2 DCM. We first used echocardiography to define the presymptomatic and symptomatic phases. Figure 1a illustrates left ventricular ejection fraction (LVEF) and diastolic diameter (LVDd) of F1B (normal control) and TO2 (DCM) hamsters at 1, 4, and 8 months of age, showing that the TO2 hamster heart at 1 month is functionally normal, in agreement with previous studies [18, 27]. LVEF and LVDd of TO2 hamsters deteriorated by approximately 25 and 5% at 4 months, respectively, and continued to deteriorate with aging. We further examined circulating biomarkers for signs of tissue damage. As shown in Fig. 1b, the 1-month TO2 hamsters exhibited normal circulating levels of serum glutamic oxaloacetic transaminase (SGOT) and lactate dehydrogenase (LDH). Consistent with the echocardiographic analysis, the 4-month TO2 hamsters exhibited elevated levels of SGOT and LDH, indicating signs of tissue damage (Fig. 1b). These results are in agreement with published histological findings [27]. We thus refer the 1- and 4-month stages as the presymptomatic and symptomatic phases of hamster DCM.

Oxidative stress at the presymptomatic stage

Although the 1-month TO2 hamster heart appeared largely normal, early subtle biochemical pathogenesis might be occurring that was not revealed by the above analyses. Plasma samples from 1-month F1B and TO2 hamsters were therefore screened by multiplexed immunoassays examining ~70 circulating biomarkers, among which the neutrophil enzyme myeloperoxidase and the inflammatory cytokine monocyte chemotactic protein-1 were significantly elevated in the asymptomatic TO2 hamsters (data not shown). Since activities of these two proteins can cause oxidative stress [28], we measured plasma concentrations of malondialdehyde (MDA), which represents the end-product of lipid peroxidation [29]. Figure 2a shows that circulating MDA levels increased with age (from 1 to 4 months) in both F1B and TO2 hamsters. Notably, TO2 hamsters exhibited significantly higher plasma MDA levels than F1B hamsters at 1 month only. Analysis of tissue MDA reveals that heart tissues from both strains at 1 month of age accumulated higher levels of MDA than skeletal muscle and liver tissues (Fig. 2b). These biochemical assays thus uncover early oxidative stress predominantly affecting the TO2 heart at the presymptomatic stage.

DCM heart expresses osteogenic markers at the presymptomatic stage

Oxidative stress-induced molecular signaling has recently been shown to activate osteogenic differentiation of vascular smooth muscle cells [30]. Circulating osteopontin and alkaline phosphatase (ALP) are sensitive osteogenic markers that are of diagnostic value [30,31]. Figure 3a shows that plasma osteopontin levels and ALP activities were significantly higher in both 1- and 4-month TO2 hamsters, suggesting ongoing abnormal osteogenic events. Heart ALP activities were further analyzed, and found to be significantly higher in both 1- and 4-month TO2 hearts (Fig. 3b). These analyses indicate early aberrant activation of an osteogenic pathway in the TO2 heart before the onset of cardiac dysfunction, and the abnormal osteogenic phenotype persisted after the manifestation of DCM.

TO2 hamsters exhibit an abnormal hormonal profile

The UM-X7.1 cardiomyopathic hamster strain has previously been found to exhibit insulin deficiency and reduced expression of lipogenic enzymes [32]. Since altered energy metabolism may have a substantial role in the development of DCM [14,15], we next investigated whether

regulation of energy metabolism in the TO2 cardiomyopathic hamster strain might be altered. Insulin and leptin are two key hormones involved in regulation of whole body metabolism. Interestingly, immunoassays revealed abnormally low levels of plasma insulin and leptin in 1-month TO2 hamsters (Fig. 4a). The observed insulin abnormality appeared transient as it became normalized at 4 months of age. The leptin abnormality on the other hand persisted from 1 to 4 months of age (Fig. 4a). Despite the transient insulin abnormality, the TO2 hamsters exhibited normal blood glucose levels at both 1 and 4 months of age (Fig. 4b).

Selective downregulation of aerobic glucose metabolism at the symptomatic stage

Early insulin abnormality at the presymptomatic stage can potentially have a long-term effect on energy metabolism, leading to subsequent left ventricular pump failure. Pyruvate dehydrogenase (PDH) complex catalyzes the rate-limiting step in aerobic glucose metabolism, and the E1 subunit of the enzyme complex is normally activated by insulin [33,34]. We carried out enzyme activity assays examining ventricular PDH activities at 1 and 4 months. Figure 5a shows that F1B and TO2 ventricular homogenates exhibited similar PDH activities at the presymptomatic stage (1 month). Interestingly, a prominent age-dependent increase in PDH activities was noted in the F1B but not TO2 samples, resulting in a ~40% lower TO2 PDH activities at the symptomatic stage (4 month). Decreased PDH activities were not observed in the TO2 muscle and liver samples (data not shown). We also assayed two additional enzymes involved in energy metabolism. Figure 5b shows that F1B and TO2 hearts exhibited similar activities of glyceraldehyde-3-phosphate dehydrogenase (GAPDH) and cytochrome *c* oxidase (COX) activities from 1 to 4 months, indicating that the observed downregulation of PDH activity in the heart of 4-month TO2 hamsters is mechanistically unique and significant.

Downregulated expression of PDH E1 subunit at the symptomatic stage

Since the E1 subunit of PDH catalyzes the rate-limiting step, and its expression is regulated by insulin [33,34], we examined the amount of the E1 subunit by Western blotting. Figure 6a shows that ventricular tissues from 1-month F1B and TO2 hamsters contained similar amount of E1 protein, which is consistent with the enzyme activity assay shown in Fig. 5. Ventricular tissues from 4-month F1B hamsters exhibited significantly higher levels of E1 protein than those from 4-month TO2 hamsters, which again is consistent with the enzyme activity assay. Expression of the 39-kD subunit of the electron transport chain complex I was also examined as internal reference, and found to be similar in F1B and TO2 samples (Fig. 6a). Densitometric quantification of the Western blots revealed a ~20% decrease in PDH E1 protein in the ventricles of 4-month TO2 hamsters (Fig. 6b). Thus, lower PDH activities in the 4-month TO2 myocardium are caused at least in part by downregulated expression of the PDH E1 subunit.

Discussion

The present study was undertaken to identify early biochemical pathogenesis in the TO2 hamster model of DCM, which exhibits cardiac dysfunction between 1 and 2 months of age and later develops congestive heart failure resembling that seen in many patients [35,36]. We found that oxidative stress, osteogenic phenotype, and energy metabolism are differentially involved in the initiation and progression of the disease. Although TO2 hamsters at 1 month of age are functionally normal and exhibit little histological abnormalities, signaling pathways may be altered at the early presymptomatic stage that are likely to be mechanistically and clinically significant.

δ-Sarcoglycan is a component of the multifunctional dystrophin-associated glycoprotein complex, which provides mechanical strength and mediates signal transduction in the cell [19,21,37]. Since loss of δ-sarcoglycan protein destabilizes the dystrophin complex, the signaling linkage between the cytoskeletal network and extracellular matrix is expected to be

altered in δ-sarcoglycan-deficient tissue. δ-Sarcoglycan has been shown to interact physically with the β1-integrin signaling molecule and mediate cell adhesion [38,39]. Along this line, we note that metabolic and signaling abnormalities have been demonstrated in the dystrophin-deficient mouse heart prior to the onset of overt cardiomyopathy [40]. These molecular events may be mediated by lipid peroxidation as evidenced here by increased concentrations of MDA, myeloperoxidase, and monocyte chemotactic protein-1 in 1-month TO2 hamsters. Myeloperoxidase, in particular, has been linked to the production of prothrombogenic oxidized lipids [41], and high levels of myeloperoxidase are detected in patients with angiographically documented cardiovascular disease and culprit lesions prone to rupture [42,43].

Oxidative stress-induced signaling has recently been shown to activate osteogenic differentiation of vascular smooth muscle cells [30]. A commonly used osteogenic marker is the phosphate-splitting enzyme alkaline phosphatase (ALP), which is induced during the early stage of osteogenesis [30,31]. Although aberrant circulating levels of ALP can be associated with a wide range of disease conditions [44,45], the abnormally high levels of ALP activities in the plasma and heart tissue of TO2 hamsters were detected in the absence of abnormal liver ALP activity. It should be mentioned that tissue calcification has been reported to be dependent on ALP activity [46], and calcified lesions are commonly present in cardiomyopathic animals and patients [19,46,47]. Thus, cardiovascular calcification may be secondary to early presymptomatic activation of ALP. It is tempting to speculate that abnormally active Wnt/β-catenin signaling may have a role in the early myocardial osteogenic phenotype since the signaling pathway is known to promote osteogenesis of mesenchymal tissue [48], and appears to be more active in the TO2 myocardium [49].

Understanding of cardiac metabolism can provide a new approach to the treatment of heart failure. Abnormalities in energetics are now considered an integral part of the primary heart muscle disease. Compromise of myocardial energy production pathways is thus expected to have a causal role in cardiomyopathies [50,51]. The UM-X7.1 cardiomyopathic hamster strain has previously been found to exhibit insulin deficiency and reduced expression of lipogenic enzymes [32]. Although the cause of insulin dysfunction in the UM-X7.1 and TO2 strains remains unclear, it may be associated with additional mutation in these animals [52]. The present study shows that compromised glucose oxidative metabolism in the TO2 heart is caused by reduced expression and activity of the E1 subunit of PDH, which may be mediated by transient low insulin levels in TO2 hamsters. This altered PDH control in hamster DCM was also recognized previously [53]. Along this line, we note that GLUT4 knockout mice were found to exhibit depressed systolic function and eventually progress to DCM [54]. These findings suggest a potentially common myocardial maladaptation process involving glucose metabolism during the development of DCM, ultimately leading to ventricular pump failure. Notably, PDH deficiency in the TO2 heart was not detected at 1 month during which time ALP elevation and lipid per-oxidation were already precipitated, suggesting that it likely contributes to the progression rather than initiation of hamster DCM.

In summary, the present study delineates an early pathogenic role of oxidative stress and osteogenic phenotype at the presymptomatic stage of δ-sarcoglycan-null DCM. The symptomatic phase is marked by reduced expression and activity of PDH E1 subunit, which is expected to impair aerobic glucose metabolism. Differential involvement of oxidative stress, osteogenic phenotype, and glucose metabolism identify important dynamic venues, which may be therapeutically targeted for early diagnosis, prevention, and treatment of human DCM.

Acknowledgments

This work was supported by NIH R01HL84590.

References

1. Richardson P, McKenna W, Bristow M, Maisch B, Mautner B, O'Connell J, et al. Report of the 1995 World Health Organization/International Society and Federation of Cardiology Task Force on the definition and classification of cardiomyopathies. Circulation 1996;93:841–842. [PubMed: 8598070]
2. Kasper EK, Agema WR, Hutchins GM, Deckers JW, Hare JM, Baughman KL. The causes of dilated cardiomyopathy: a clinicopathologic review of 673 consecutive patients. J Am Coll Cardiol 1994;23:586–590. [PubMed: 8113538]
3. Shaw T, Elliott P, McKenna WJ. Dilated cardiomyopathy: a genetically heterogeneous disease. Lancet 2002;360:654–655. doi:10.1016/S0140-6736(02)09879-3. [PubMed: 12241867]
4. Perriard JC, Hirschy A, Ehler E. Dilated cardiomyopathy: a disease of the intercalated disc? Trends Cardiovasc Med 2003;13:30–38. doi:10.1016/S1050-1738(02)00209-8. [PubMed: 12554098]
5. Fatkin D, Graham RM. Molecular mechanisms of inherited cardiomyopathies. Physiol Rev 2002;82:945–980. [PubMed: 12270949]
6. Towbin JA, Bowles NE. Dilated cardiomyopathy: a tale of cytoskeletal proteins and beyond. J Cardiovasc Electrophysiol 2006;17:919–926. doi:10.1111/j.1540-8167.2006.00530.x. [PubMed: 16764708]
7. Mason JW. Myocarditis and dilated cardiomyopathy: an inflammatory link. Cardiovasc Res 2003;60:5–10. doi:10.1016/S0008-6363(03)00437-1. [PubMed: 14522402]
8. Maisch B, Richter A, Sandmoller A, Portig I, Pankuweit S. Inflammatory dilated cardiomyopathy (DCMI). Herz 2005;30:535–544. doi:10.1007/s00059-005-2730-5. [PubMed: 16170686]
9. Ashrafian H, Watkins H. Reviews of translational medicine and genomics in cardiovascular disease: new disease taxonomy and therapeutic implications cardiomyopathies: therapeutics based on molecular phenotype. J Am Coll Cardiol 2007;49:1251–1264. doi:10.1016/j.jacc.2006.10.073. [PubMed: 17394955]
10. Mavroidis M, Capetanaki Y. Extensive induction of important mediators of fibrosis and dystrophic calcification in desmin-deficient cardiomyopathy. Am J Pathol 2002;160:943–952. [PubMed: 11891192]
11. Thornell L, Carlsson L, Li Z, Mericskay M, Paulin D. Null mutation in the desmin gene gives rise to a cardiomyopathy. J Mol Cell Cardiol 1997;29:2107–2124. doi:10.1006/jmcc.1997.0446. [PubMed: 9281443]
12. Ashrafian H, Redwood C, Blair E, Watkins H. Hypertrophic cardiomyopathy: a paradigm for myocardial energy depletion. Trends Genet 2003;19:263–268. doi:10.1016/S0168-9525(03)00081-7. [PubMed: 12711218]
13. Crilley JG, Boehm EA, Blair E, Rajagopalan B, Blamire AM, Styles P, et al. Hypertrophic cardiomyopathy due to sarcomeric gene mutations is characterized by impaired energy metabolism irrespective of the degree of hypertrophy. J Am Coll Cardiol 2003;41:1776–1782. doi:10.1016/S0735-1097(02)03009-7. [PubMed: 12767664]
14. Arbustini E, Diegoli M, Fasani R, Grasso M, Morbini P, Banchieri N, et al. Mitochondrial DNA mutations and mitochondrial abnormalities in dilated cardiomyopathy. Am J Pathol 1998;153:1501–1510. [PubMed: 9811342]
15. Santorelli FM, Tanji K, Manta P, Casali C, Krishna S, Hays AP, et al. Maternally inherited cardiomyopathy: an atypical presentation of the mtDNA 12S rRNA gene A1555G mutation. Am J Hum Genet 1999;64:295–300. doi:10.1086/302188. [PubMed: 9915970]
16. Giordano FJ. Oxygen, oxidative stress, hypoxia, and heart failure. J Clin Invest 2005;115:500–508. [PubMed: 15765131]
17. Minieri M, Fiaccavento R, Carosella L, Peruzzi G, Di Nardo P. The cardiomyopathic hamster as model of early myocardial aging. Mol Cell Biochem 1999;198:1–6. doi:10.1023/A:1006926411659. [PubMed: 10497872]
18. Goineau S, Pape D, Guillo P, Ramee M-P, Bellissant E. Hemodynamic and histomorphometric characteristics of dilated cardiomyopathy of Syrian hamsters (Bio TO-2 strain). Can J Physiol Pharmacol 2001;79:329–337. doi:10.1139/cjpp-79-4-329. [PubMed: 11332510]
19. Sakamoto A, Ono K, Abe M, Jasmin G, Eki T, Murakami Y, et al. Both hypertrophic and dilated cardiomyopathies are caused by mutation of the same gene, delta-sarcoglycan, in hamster: an animal

model of disrupted dystrophin-associated glycoprotein complex. Proc Natl Acad Sci USA 1997;94:13873–13878. doi:10.1073/pnas.94.25.13873. [PubMed: 9391120]

20. Dhalla NS, Panagia V, Makino N, Beamish RE. Sarcolemmal Na^{+}–Ca^{2+} exchange and Ca^{2+}-pump activities in cardiomyopathies due to intracellular Ca^{2+}-overload. Mol Cell Biochem 1988;82:75–79. doi:10.1007/BF00242519. [PubMed: 2972915]
21. Coral-Vazquez R, Cohn RD, Moore SA, Hill JA, Weiss RM, Davisson RL, et al. Disruption of the sarcoglycan–sarcospan complex in vascular smooth muscle: a novel mechanism for cardiomyopathy and muscular dystrophy. Cell 1999;98:465–474. doi:10.1016/S0092-8674(00)81975-3. [PubMed: 10481911]
22. Wheeler MT, Allikian MJ, Heydemann A, Hadhazy M, Zarnegar S, McNally EM. Smooth muscle cell-extrinsic vascular spasm arises from cardiomyocyte degeneration in sarcoglycan-deficient cardiomyopathy. J Clin Invest 2004;113:668–675. [PubMed: 14991064]
23. Nigro V, de Sa Moreira E, Piluso G, Vainzof M, Belsito A, Politano L, et al. Autosomal recessive limb-girdle muscular dystrophy, LGMD2F, is caused by a mutation in the delta-sarcoglycan gene. Nat Genet 1996;14:195–198. doi:10.1038/ng1096-195. [PubMed: 8841194]
24. Jung D, Duclos F, Apostol B, Straub V, Lee JC, Allamand V, et al. Characterization of delta-sarcoglycan, a novel component of the oligomeric sarcoglycan complex involved in limb-girdle muscular dystrophy. J Biol Chem 1996;271:32321–32329. doi:10.1074/jbc.271.50.32321. [PubMed: 8943294]
25. Kositprapa C, Zhang B, Berger S, Canty JMJ, Lee TC. Calpain-mediated proteolytic cleavage of troponin I induced by hypoxia or metabolic inhibition in cultured neonatal cardiomyocytes. Mol Cell Biochem 2000;214:47–55. doi:10.1023/A:1007160702275. [PubMed: 11195789]
26. Lin H, Shabbir A, Molnar M, Lee T. Stem cell regulatory function mediated by expression of a novel mouse Oct4 pseudogene. Biochem Biophys Res Commun 2007;355:111–116. doi:10.1016/j.bbrc.2007.01.106. [PubMed: 17280643]
27. Nishizawa T, Iwase M, Kanazawa H, Ichihara S, Ichihara G, Nagata K, et al. Serial alterations of beta-adrenergic signaling in dilated cardiomyopathic hamsters: possible role of myocardial oxidative stress. Circ J 2004;68:1051–1060. doi:10.1253/circj.68.1051. [PubMed: 15502388]
28. Daugherty A, Dunn JL, Rateri DL, Heinecke JW. Myeloperoxidase, a catalyst for lipoprotein oxidation, is expressed in human atherosclerotic lesions. J Clin Invest 1994;94:437–444. doi:10.1172/JCI117342. [PubMed: 8040285]
29. Casini AF, Ferrali M, Pompella A, Maellaro E, Comporti M. Lipid peroxidation and cellular damage in extrahepatic tissues of bromobenzene-intoxicated mice. Am J Pathol 1986;123:520–531. [PubMed: 3717304]
30. Byon CH, Javed A, Dai Q, Kappes JC, Clemens TL, Darley- Usmar VM, McDonald JM, Chen Y. Oxidative stress induces vascular calcification through modulation of the osteogenic transcription factor runx-2 by akt signaling. J Biol Chem 2008;283:15319–15327. [PubMed: 18378684]
31. Stinson RA, Hamilton BA. Human liver plasma membranes contain an enzyme activity that removes membrane anchor from alkaline phosphatase and converts it to a plasma-like form. Clin Biochem 1994;27:49–55. doi:10.1016/0009-9120(94)90011-6. [PubMed: 8200115]
32. Vecchini A, Binaglia L, Bibeau M, Minieri M, Carotenuto F, Di Nardo P. Insulin deficiency and reduced expression of lipogenic enzymes in cardiomyopathic hamster. J Lipid Res 2001;42:96–105. [PubMed: 11160370]
33. Patel MS, Korotchkina LG. Regulation of the pyruvate dehydrogenase complex. Biochem Soc Trans 2006;34:217–222. doi:10.1042/BST20060217. [PubMed: 16545080]
34. Harris RA, Bowker-Kinley MM, Huang B, Wu P. Regulation of the activity of the pyruvate dehydrogenase complex. Adv Enzyme Regul 2002;42:249–259. doi:10.1016/S0065-2571(01)00061-9. [PubMed: 12123719]
35. Panchal BC, Trippodo NC. Systemic and regional hemodynamics in conscious BIO TO-2 cardiomyopathic hamsters. Cardiovasc Res 1993;27:2264–2269. doi:10.1093/cvr/27.12.2264. [PubMed: 8313437]
36. Ryoke T, Gu Y, Ikeda Y, Martone ME, Oh SS, Jeon ES, et al. Apoptosis and oncosis in the early progression of left ventricular dysfunction in the cardiomyopathic hamster. Basic Res Cardiol 2002;97:65–75. doi:10.1007/s395-002-8389-4. [PubMed: 12004790]

37. Rando TA. The dystrophin-glycoprotein complex, cellular signaling, and the regulation of cell survival in the muscular dystrophies. Muscle Nerve 2001;24:1575–1594. doi:10.1002/mus.1192. [PubMed: 11745966]
38. Yoshida T, Pan Y, Hanada H, Iwata Y, Shigekawa M. Bidirectional signaling between sarcoglycans and the integrin adhesion system in cultured L6 myocytes. J Biol Chem 1998;273:1583–1590. doi: 10.1074/jbc.273.3.1583. [PubMed: 9430699]
39. Skinner MA, Wildeman AG. Beta(1) integrin binds the 16-kDa subunit of vacuolar H(+)-ATPase at a site important for human papillomavirus E5 and platelet-derived growth factor signaling. J Biol Chem 1999;274:23119–23127. doi:10.1074/jbc.274.33.23119. [PubMed: 10438481]
40. Khairallah M, Khairallah R, Young ME, Dyck JR, Petrof BJ, Des Rosiers C. Metabolic and signaling alterations in dystrophin-deficient hearts precede overt cardiomyopathy. J Mol Cell Cardiol 2007;43:119–129. doi:10.1016/j.yjmcc.2007.05.015. [PubMed: 17583724]
41. Podrez EA, Poliakov E, Shen Z, Zhang R, Deng Y, Sun M, et al. Identification of a novel family of oxidized phospholipids that serve as ligands for the macrophage scavenger receptor CD36. J Biol Chem 2002;277:38503–38516. doi:10.1074/jbc.M203318200. [PubMed: 12105195]
42. Zhang R, Brennan ML, Fu X, Aviles RJ, Pearce GL, Penn MS, et al. Association between myeloperoxidase levels and risk of coronary artery disease. JAMA 2001;286:2136–2142. doi: 10.1001/jama.286.17.2136. [PubMed: 11694155]
43. Sugiyama S, Okada Y, Sukhova GK, Virmani R, Heinecke JW, Libby P. Macrophage myeloperoxidase regulation by granulocyte macrophage colony-stimulating factor in human atherosclerosis and implications in acute coronary syndromes. Am J Pathol 2001;158:879–891. [PubMed: 11238037]
44. Wolf PL. Clinical significance of an increased or decreased serum alkaline phosphatase level. Arch Pathol Lab Med 1978;102:497–501. [PubMed: 30431]
45. Christenson RH. Biochemical markers of bone metabolism: an overview. Clin Biochem 1997;30:573–593. doi:10.1016/S0009-9120(97)00113-6. [PubMed: 9455610]
46. Mathieu P, Voisine P, Pepin A, Shetty R, Savard N, Dagenais F. Calcification of human valve interstitial cells is dependent on alkaline phosphatase activity. J Heart Valve Dis 2005;14:353–357. [PubMed: 15974530]
47. Fiaccavento R, Carotenuto F, Minieri M, Fantini C, Forte G, Carbone A, et al. Stem cell activation sustains hereditary hypertrophy in hamster cardiomyopathy. J Pathol 2005;205:397–407. doi: 10.1002/path.1717. [PubMed: 15682436]
48. Caverzasio J, Manen D. Essential role of Wnt3a-mediated activation of mitogen-activated protein kinase p38 for the stimulation of alkaline phosphatase activity and matrix mineralization in C3H10T1/2 mesenchymal cells. Endocrinology 2007;148:5323–5330. doi:10.1210/en.2007-0520. [PubMed: 17717053]
49. Masuelli L, Bei R, Sacchetti P, Scappaticci I, Francalanci P, Albonici L, et al. Beta-catenin accumulates in intercalated disks of hypertrophic cardiomyopathic hearts. Cardiovasc Res 2003;60:376–387. doi:10.1016/j.cardiores.2003.08.005. [PubMed: 14613867]
50. Neubauer S. The failing heart—an engine out of fuel. N Engl J Med 2007;356:1140–1151. doi: 10.1056/NEJMra063052. [PubMed: 17360992]
51. Ingwall JS, Weiss RG. Is the failing heart energy starved? On using chemical energy to support cardiac function. Circ Res 2004;95:135–145. doi:10.1161/01.RES.0000137170.41939.d9. [PubMed: 15271865]
52. Minieri M, Zingarelli M, Shubeita H, Vecchini A, Binaglia L, Carotenuto F, et al. Identification of a new missense mutation in the mtDNA of hereditary hypertrophic, but not dilated cardiomyopathic hamsters. Mol Cell Biochem 2003;252:73–81. doi:10.1023/A:1025542731335. [PubMed: 14577578]
53. Di Lisa F, Fan CZ, Gambassi G, Hogue BA, Kudryashova I, Hansford RG. Altered pyruvate dehydrogenase control and mitochondrial free Ca^{2+} in hearts of cardiomyopathic hamsters. Am J Physiol 1993;264:H2188–H2197. [PubMed: 8322950]
54. Stenbit AE, Katz EB, Chatham JC, Geenen DL, Factor SM, Weiss RG, et al. Preservation of glucose metabolism in hypertrophic GLUT4-null hearts. Am J Physiol Heart Circ Physiol 2000;279:H313–H318. [PubMed: 10899071]

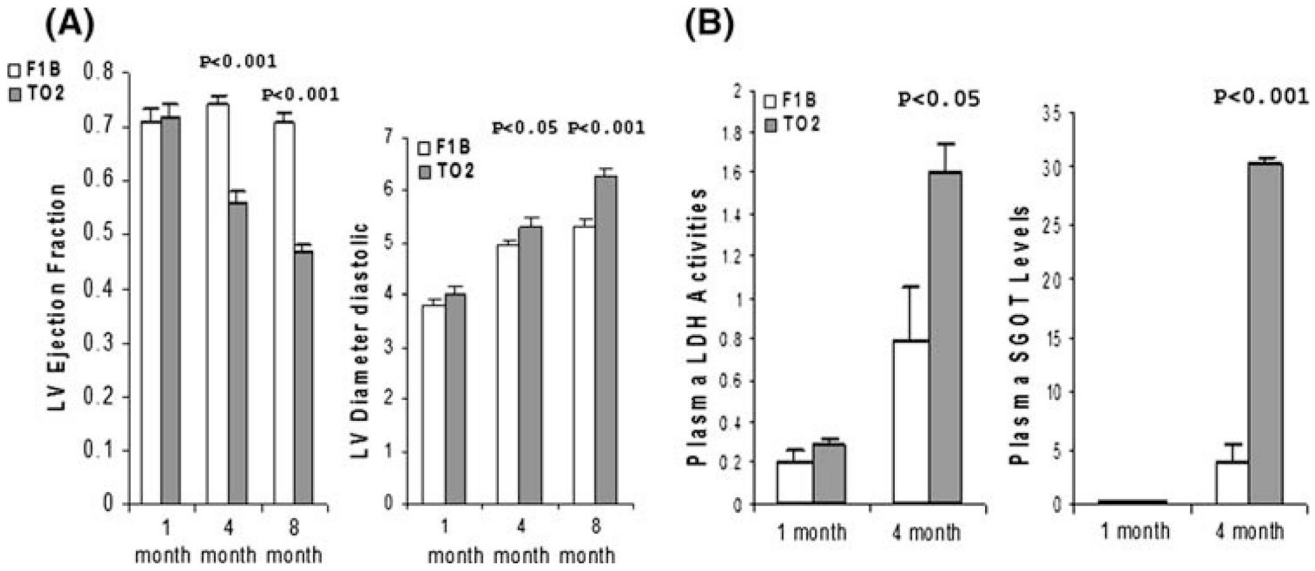

Fig. 1.

Presymptomatic and symptomatic stages of TO2 hamster DCM defined by physiological and biochemical measures. (**a**) Echocardiographic measurements of LVEF and LVDd at 1, 4, and 8 months of age ($n = 5$ for each time point). (**b**) Plasma samples from F1B and TO2 hamsters were assayed for LDH enzyme activities (expressed as relative O.D. units) and SGOT levels (expressed as μg/ml). Each time point was from $n = 3$. Results were means ± SEM. *P* values shown were comparisons between F1B and TO2 hamsters as Indicated

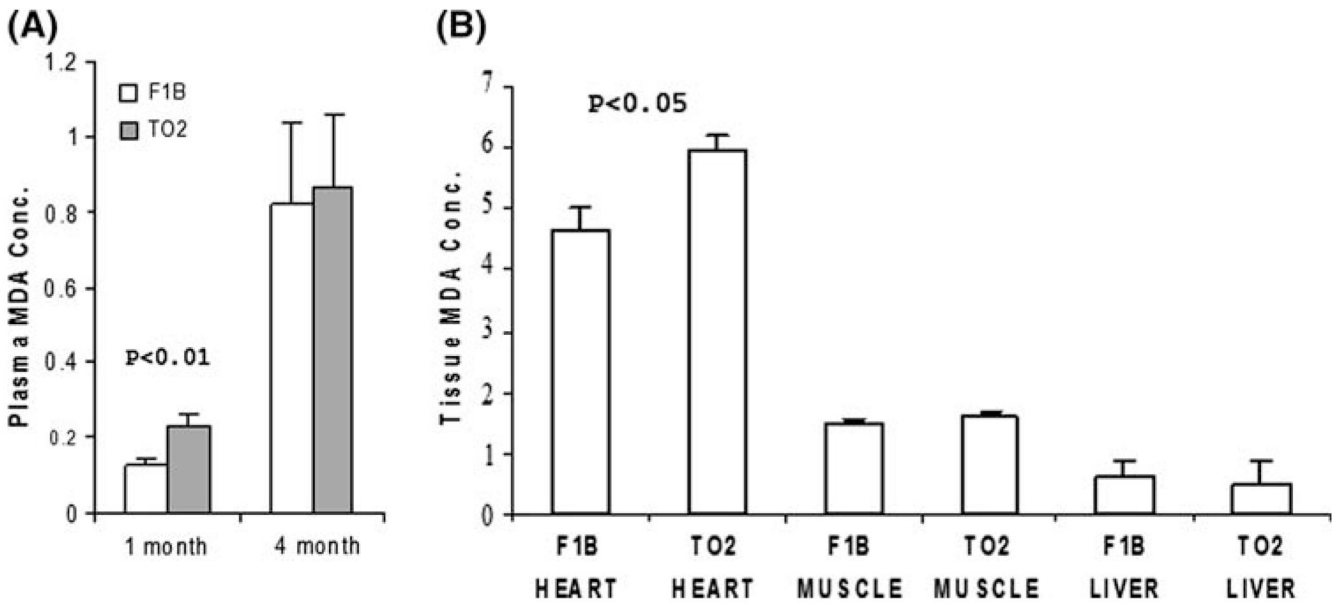

Fig. 2.

TO2 hamster DCM exhibits presymptomatic oxidative stress. MDA assays were performed as described [25] using plasma (**a**) and tissue homogenates (**b**) from 1-month hamsters ($n = 3$ for each bar). MDA concentrations (μM) shown were means ± SEM. *P* values shown were comparisons between F1B and TO2 as indicated

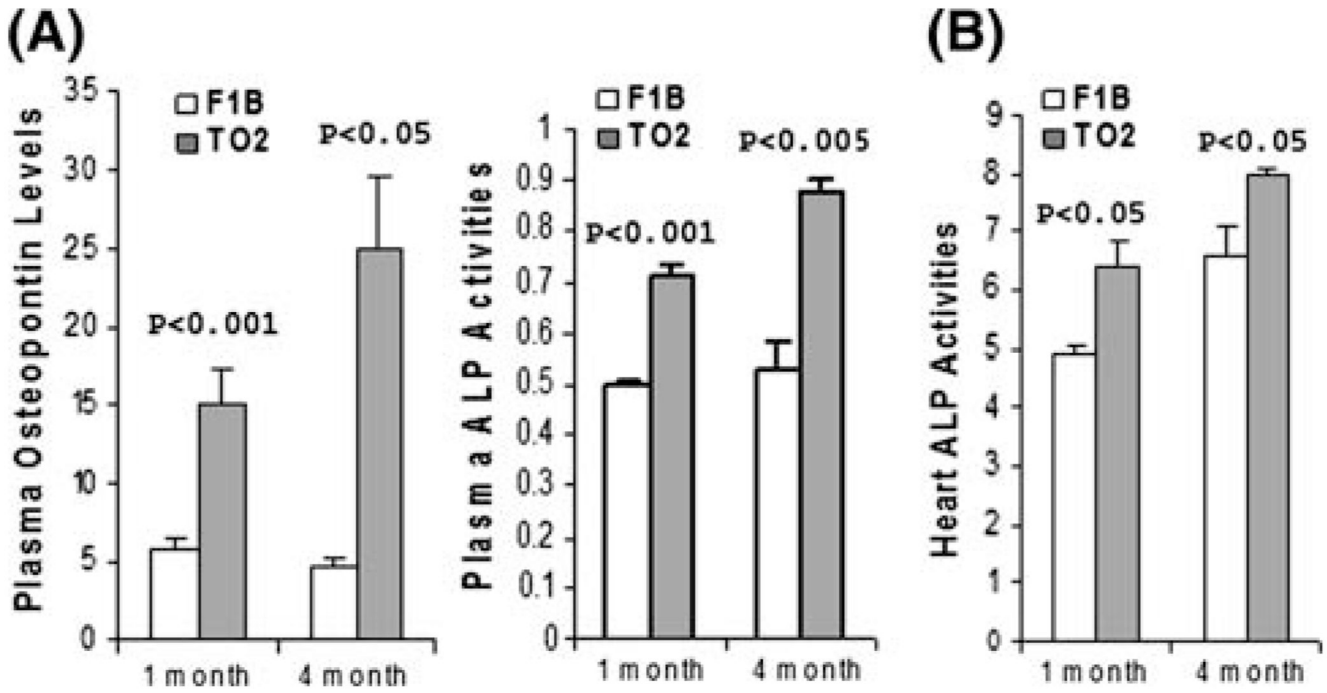

Fig. 3.

TO2 hamster DCM exhibits presymptomatic osteogenic phenotype. (**a**) Plasma osteopontin levels (ng/ml) were determined by MAP analysis ($n = 3$ for each time point). Plasma ALP activities (O.D. units) were determined enzymatically using *p*-nitrophenyl phosphate as substrate ($n = 3$ for each time point). (**b**) Heart ALP activities (expressed as O.D. units per mg proteins) were enzymatically assayed as described. Data shown were means ± SEM. *P* values shown were comparisons between F1B and TO2 hamsters

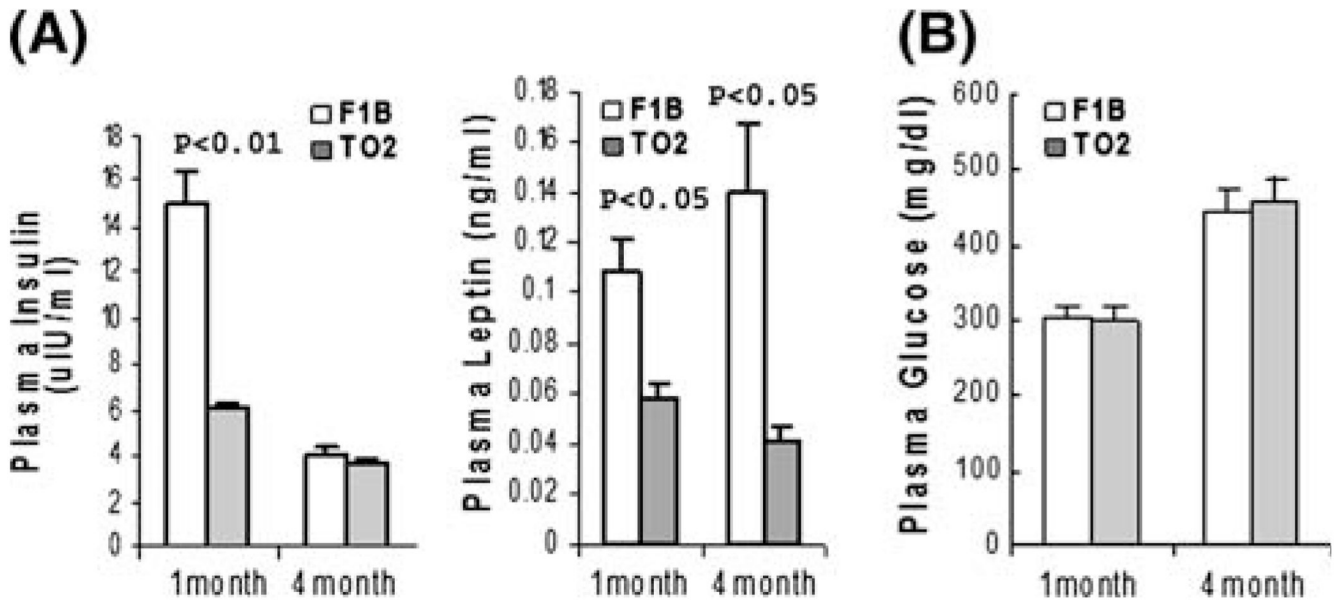

Fig. 4.

Abnormal regulation of insulin and leptin in TO2 hamsters. (**a**) Plasma levels of insulin (uIU/ml) and leptin (ng/ml) were determined by the MAP analysis. (**b**) Plasma glucose concentrations (mg/dL) were determined using the OneTouch glucose strips. All data were from $n = 3$. Data shown were means ± SEM. *P* values shown were comparisons between F1B and TO2 hamsters as indicated

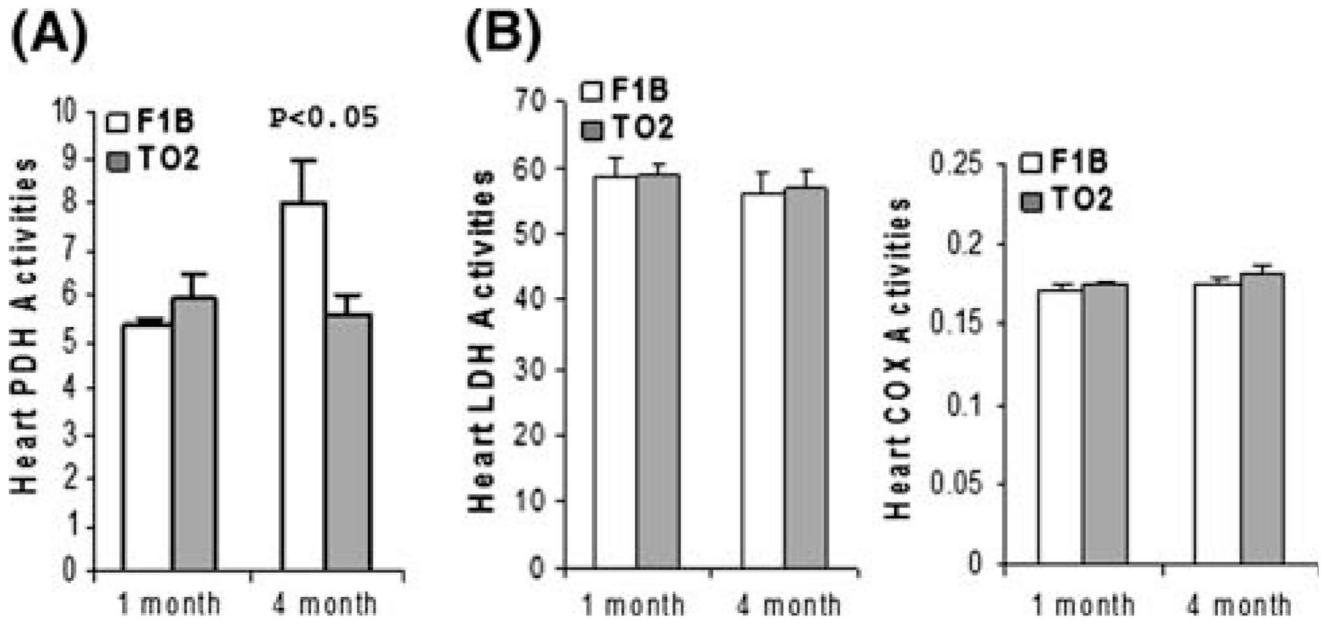

Fig. 5.

The symptomatic stage of TO2 DCM is associated with downregulation of heart pyruvate dehydrogenase (PDH) activity. Tissue homogenates were prepared from ventricular tissue at 1 and 4 months (n = 3 for each time point). Pelleted membrane fractions were used for PDH assay (**a**) and COX assay (**b**). Soluble fractions were used for LDH assay (**b**) PDH and LDH enzyme activities (expressed as O.D. units per mg proteins) were normalized by total protein concentrations. COX enzyme activities were expressed as units/ml. Results were means ± SEM. P values were comparison between F1B and TO2 at the time point indicated. Muscle and liver PDH activities were also measured, and were found to be similar between F1B and TO2 hamsters (data not shown)

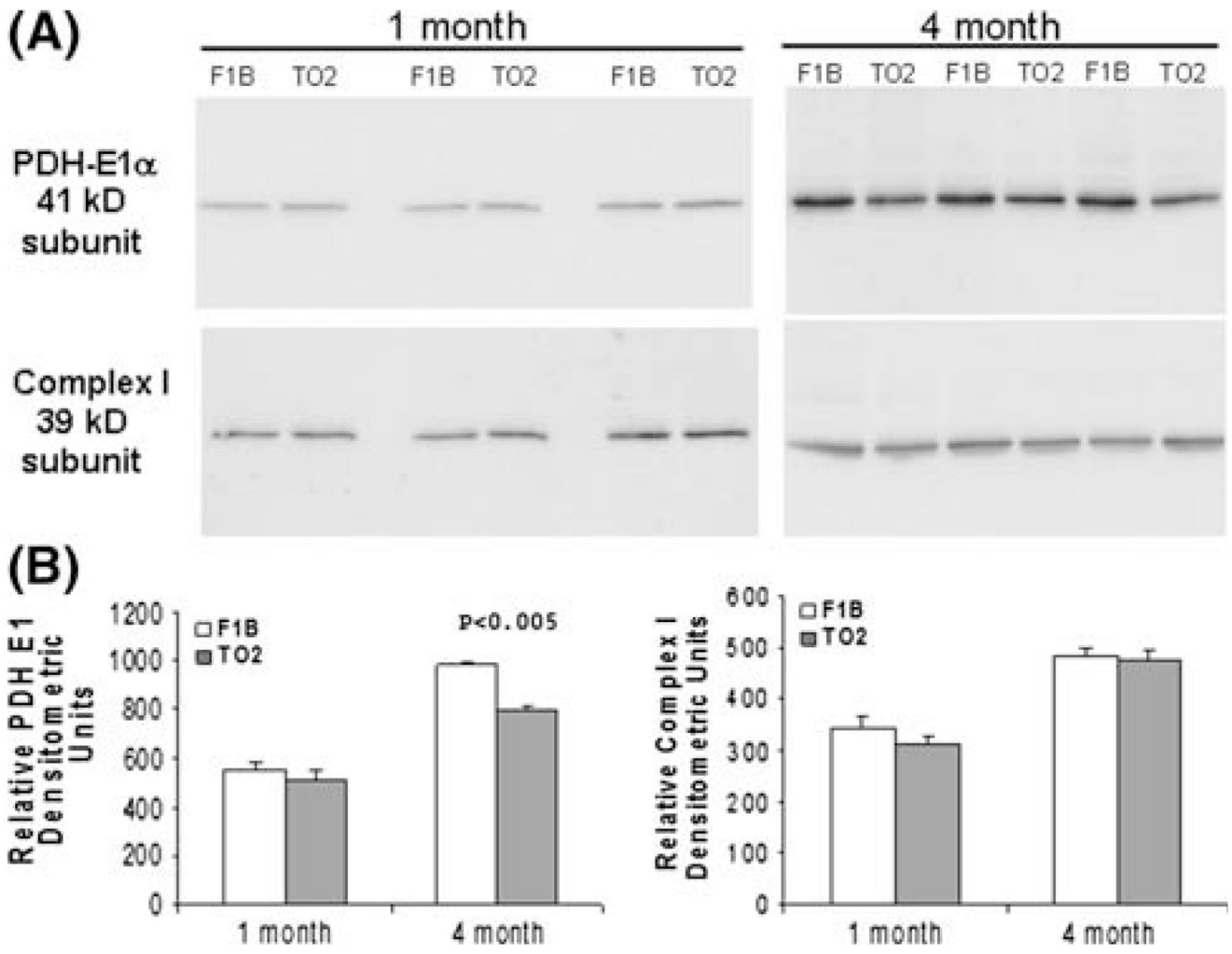

Fig. 6.

Downregulated PDH activity is mediated by reduced expression of the PDH E1 subunit. (**a**) Protein samples ($n = 3$) from Fig. 5 were analyzed by SDS-PAGE followed by Western blotting using antibodies specific for PDH E1 subunit and the 39-kD subunit of the electron transport chain complex I. (**b**) Relative abundance of each detected protein band was quantified by densitometric analysis, and illustrated in arbitrary densitometric units. The *P* value shown was comparison between F1B and TO2 at the time point indicated